Atherosclerosis 365 (2023) 15–24

Contents lists available at ScienceDirect

Atherosclerosis

journal homepage: www.elsevier.com/locate/atherosclerosis

Vascular smooth muscle cells in low SYNTAX scores coronary artery disease exhibit proinflammatory transcripts and proteins correlated with IL1B activation

Rajkumar Dorajoo [a,b,1], Mario Octavianus Ihsan [c,1], Wenting Liu [a,d], Hwee Ying Lim [e], Veronique Angeli [e], Sung-Jin Park [f], Joyce M.S. Chan [f,g,h], Xiao Yun Lin [i], Mei Shan Ong [c], Umamaheswari Muniasamy [c], Chi-Hang Lee [j,k,l], Rijan Gurung [a,l], Hee Hwa Ho [m], Roger Foo [a,j,k,l], Jianjun Liu [a,j], Theo Kofidis [c,i,l], Chuen Neng Lee [c,i], Vitaly A. Sorokin [c,i,*]

[a] Genome Institute of Singapore, Agency for Science, Technology and Research (A*STAR), Singapore
[b] Health Services and Systems Research, Duke-NUS Medical School Singapore, Singapore
[c] Department of Surgery, Yong Loo Lin School of Medicine, National University of Singapore, Singapore
[d] Taihe Hospital, Hubei University of Medicine and Center of Health Administration and Development Studies, School of Public Health, Hubei University of Medicine, Singapore
[e] Immunology Translational Research Program, Department of Microbiology and Immunology, National University of Singapore, Singapore
[f] Translational Cardiovascular Imaging Group, Institute of Bioengineering and Bioimaging (IBB), Agency for Science, Technology and Research (A*STAR), Singapore
[g] Department of Vascular Surgery, Singapore General Hospital, SingHealth, Singapore
[h] Lee Kong Chian School of Medicine, Nanyang Technological University, Singapore
[i] Department of Cardiac, Thoracic and Vascular Surgery, National University Hospital, National University Health System, Singapore
[j] Department of Medicine, Yong Loo Lin School of Medicine, National University of Singapore, Singapore
[k] Department of Cardiology, National University Hospital, National University Health System, Singapore
[l] Cardiovascular Research Institute, Yong Loo Lin School of Medicine, National University of Singapore, Singapore
[m] Department of Cardiology, Tan Tock Seng Hospital, Singapore

ARTICLE INFO

Keywords:
Vascular smooth muscle cells
IL1B
SYNTAX score

ABSTRACT

Background and aims: The SYNTAX score is clinically validated to stratify number of lesions and pattern of CAD. A better understanding of the underlying molecular mechanisms influencing the pattern and complexity of coronary arteries lesions among CAD patients is needed.

Methods: Human arterial biopsies from 49 patients (16 low-SYNTAX-score (LSS, <23), 16 intermediate-SYNTAX-score (ISS, 23 to 32) and 17 high-SYNTAX-score (HSS, >32)) were evaluated using Affymetrix GeneChip® Human Genome U133 Plus 2.0 microarray. The data were validated by Next-Generation Sequencing (NGS). Primary VSMC from patients with low and high SYNTAX scores were isolated and compared using immunohistochemistry, qPCR and immunoblotting to confirm mRNA and proteomic results.

Results: The *IL1B* was verified as the top upstream regulator of 47 inflammatory DEGs in LSS patients and validated by another sets of patient samples using NGS analysis. The upregulated expression of *IL1B* was translated to increased level of IL1β protein in the LSS tissue based on immunohistochemical quantitative analysis. Plausibility of idea that *IL1B* in the arterial wall could be originated from VSMC was checked by exposing culture to proinflammatory conditions where *IL1B* came out as the top DEG (logFC = 7.083, *FDR* = 1.38×10^{-114}). The LSS patient-derived primary VSMCs confirmed higher levels of IL1B mRNA and protein.

Conclusions: LSS patients could represent a group of patients where IL1B could play a substantial role in disease pathogenesis. The LSS group could represent a plausible cohort of patients for whom anti-inflammatory therapy could be considered.

* Corresponding author. Department of Surgery, National University of Singapore, 1E Kent Ridge Road, NUHS Tower Block, Level 8, 119228, Singapore.
E-mail address: sursv@nus.edu.sg (V.A. Sorokin).
[1] These authors contributed equally to this work.

https://doi.org/10.1016/j.atherosclerosis.2022.12.005
Received 27 July 2022; Received in revised form 22 November 2022; Accepted 16 December 2022
Available online 17 December 2022

1. Introduction

The highly multifactorial nature of coronary artery disease (CAD) represents a substantial difficulty to derive the precise pathogenic mechanisms responsible for disease progression in every particular clinical case. It makes patient-specific therapy for CAD a challenging task. Although, the majority of patients would be treated for hyperlipidemia, use of anti-inflammatory medication is still a matter of clinical debate, despite multiple genetic studies showing that CAD-related genes are involved in processes related to inflammation [1,2]. An inflammatory cytokine that has recently gained prominence as therapeutic target in atherosclerosis is Interleukin-1 Beta (IL1B) [3]. IL1B has been well characterized to induce an inflammatory response in endothelial cells and promotes the accumulation and invasion of immune cells, such as inflammatory macrophages, into the local intima of blood vessels triggering a positive loop of increased inflammatory mediators and stimulation of vascular smooth muscle proliferation and differentiation [4]. The recent Canakinumab Anti-inflammatory Thrombosis Outcome Study (CANTOS) clinical study with the anti-inflammatory treatment targeting IL1B, also resulted in a modest but significant 15% reduction in the primary endpoint [5] and efforts may be required to better identify specific patient groups for such targeted anti-inflammatory interventions.

Coronary arteries imaging (angiogram) allows to calculate the number of lesions, assess pattern of disease, and hence, determine the severity of CAD with the well-validated SYNTAX score method (based on the *SYN*ergy between percutaneous coronary intervention with *TAX*us drug eluting stent and cardiac surgery trial). Several large multicenter trials have indicated that the calculated SYNTAX score (SS) based on the number of coronary lesions correlates with clinical outcome and influences interventions [6]. Currently, SS is routinely used in clinical practice to identify patients for coronary angioplasty or surgical intervention. Although, this score strongly correlates with interventional strategy, the underlying molecular mechanisms influencing the number of lesions in coronary arteries and pattern of disease, which are defined by SS, are yet to be fully understood.

Up to now, the majority of studies on severity of CAD investigated the relation between SS and changes in patients' blood (cells or plasma) [7–10]. While peripheral blood characteristics are known to correlate to CAD disease etiology to a certain extent, determining the precise disease mechanisms will require a direct and in-depth investigation of disease-relevant primary cells and tissues [11]. In this study, we acquired human arterial tissue during coronary arteries bypass grafting (CABG) surgery and evaluated the gene expression signatures of patient's arteries in association with different patterns of coronary artery lesions defined by calculated SSs. The identified top differentially expressed genes (DEGs) hits were validated and further characterized through RNA NGS, immunohistochemistry (IHC), and experimental work with primary cell cultures isolated from independent cohorts of CAD patients with different SS. The data were additionally compared to early- and late-stage mouse atherosclerosis models. The compelling evidence reveals that coronary artery lesions characterized by SS might represent different pathophysiological processes in the arterial wall at the transcriptomic and proteomic levels. Our results showed that arterial wall tissue of low-SS patients have increased proinflammatory transcripts. Moreover, we found that IL1B is top upstream regulator of identified proinflammatory pathways. Also, data revealed that IL1B-related transcript and protein levels were elevated mainly in vascular smooth muscle cells (VSMCs) of these patient with low SS. Our data correlates with recent studies on human tissue and primary human cells, which show that VSMCs are strongly related to inflammation and disease progression in CAD [12,13].

Overall, we believe that SSs might correlate with level of inflammatory changes in the arterial wall, and arterial VSMCs in particular. In our understanding, SS would rather characterize disease patterns, defined by different pathological mechanisms, where the LSS group would exhibit strong proinflammatory changes in the arterial wall.

2. Materials and methods

2.1. Clinical information and arterial wall sample collection

The workflow of the entire study is presented in Fig. 1. In brief, human arterial tissues were obtained at the discovery stage. A total of 49 patients (16 low-SYNTAX-score [LSS, <23], 16 intermediate-SYNTAX-score [ISS, 23 to 32] and 17 high-SYNTAX-score [HSS, >32]), who presented with CAD and underwent isolated coronary artery bypass graft (CABG) surgery at the National University Hospital of Singapore from 2010 to 2014, were recruited. In the validation stage, 6 additional patients (3 LSS and 3 HSS) were recruited. All patients were selected based on the following criteria: male, ethnically Chinese, age 55 to 75, no diabetes mellitus, no renal impairment, and no peripheral vascular disease. The SYNTAX score was calculated blindly by two independent medical staff members using the official online calculator (www.syntaxscore.org). Demographics and preoperative data (risk factors, lipid profile, medications) were compared and found not to be statistically significant at $p > 0.05$ (Supplementary Table 1). The study experimental design and workflow were approved by the National Healthcare Group Domain Specific Review Board (NHG DSRB Reference Number: 2014/00952). Written consent was obtained from patients prior to inclusion in the study (NHG Tissue Bank Registration Number: NUH/2009–0073).

2.2. Specimen collection and RNA processing

Aortic wall tissues were collected from all patients during their CABG surgery at the time of proximal anastomosis between the aorta and saphenous vein grafts. The tissues were cryopreserved on dry ice immediately before transfer to a liquid nitrogen tank for storage. Total RNA was isolated using a miRCURY™ RNA Isolation Kit – Tissue (Exiqon, Denmark) following the manufacturer's protocol. Quantification of the total RNA isolated was performed with a Thermo Scientific™ NanoDrop 8000 (Thermo Fisher Scientific, MA, USA), and quality assessment was performed using an Agilent 2100 Bioanalyzer (Agilent Technology, USA) with an Agilent RNA 6000 Pico Kit.

2.3. Microarray gene expression analysis

Total RNA from aortic wall tissues from the 49 discovery-stage CAD patients was extracted for microarray analysis. Sample quality was assessed with a NanoDrop™ 8000 Spectrophotometer (Thermo Fisher Scientific, MA, USA) and an Agilent RNA 6000 Pico Kit (Agilent), which was run on an Agilent Technologies 2100 Bioanalyzer. Microarray studies were performed using an Affymetrix GeneChip® Human Genome U133 Plus 2.0 Array for mRNA with standard operating procedures and quality control described by the manufacturer's protocol. Samples from different SS groups were randomized to prevent batch effects, and sample processing was performed simultaneously to minimize variation.

Quality control of the microarray data was performed using the Transcriptome Analysis Console (TAC). Two samples from the HSS group, 1 from the LSS group and 1 from the ISS group were identified with poor labeling of control data and were excluded from subsequent analysis (Supplementary Figs. 1A and B). For every mRNA expression probe set, normalization, background subtraction, and expression summarization were performed using the robust multi-array average (RMA) approach [14]. Quantile normalization followed by a median polish was used to remove probe affinity effects when calculating probe set summaries. The expression value was the $\log_2$ of the signal intensity. Low-expression probe sets were removed if not expressed in more than 25% of the samples. The expression level of each gene was estimated by calculating the median of the expression levels of all the probes mapped within the coding region of the gene (HG19). Batch effects were adjusted

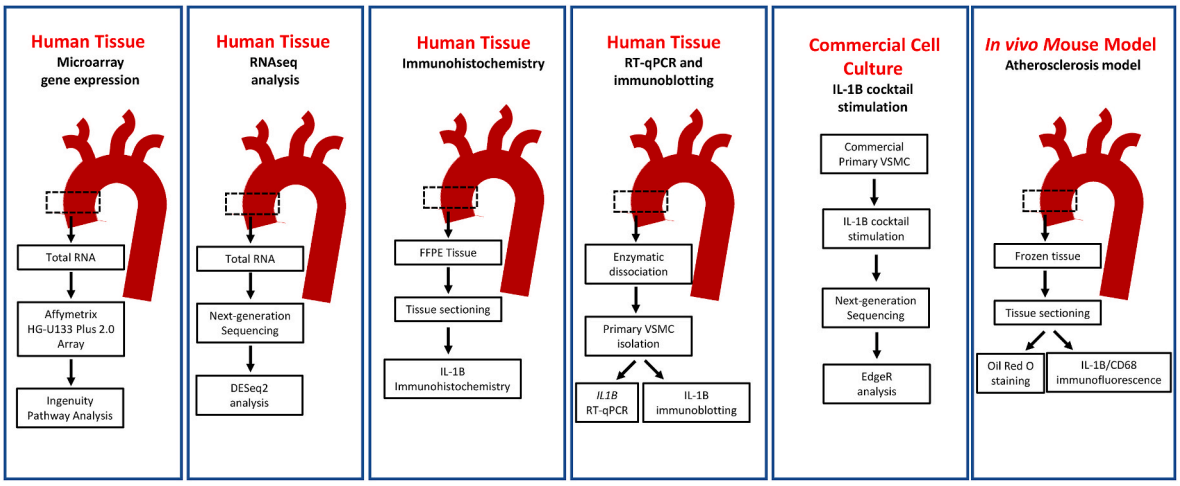

Fig. 1. Study experimental design and workflow.

using the "combat" R package [15] and age, hypertension, hyperlipidemia, and hidden variables detected by surrogate variable analysis (SVA) [16] were adjusted with "snm" [17]. The residual normalized gene expression was fit into a regression model with the R package "limma" [18]. To improve power in the discovery analysis to identify DEGs, comparisons were performed using groups with more extreme SS (i.e. HSS as compared to LSS groups). A moderated *t*-test was adopted to identify the DEGs between HSS and LSS patient groups. Genes with a Benjamini–Hochberg-adjusted *p* value (p_{Adj}) < 0.05 and with at least a 1.5-fold change (FC) were determined to be significant DEGs.

The GeneCards database (https://www.genecards.org/) was utilized to identify all prior "coronary artery disease"-related genes (6997 genes with >0 relevance score). These genes were subsequently overlapped with the identified DEGs in the study. Pathway-based analysis and upstream target analyses for the identified DEGs were performed using Ingenuity Pathway Analysis (IPA) (ver60467501). Interconnected genes were identified in IPA according to all direct and indirect interactions of activation, expression, inhibition, transcription and protein–protein interactions using the Path Explorer and Connect functions (Fig. 2A–C).

2.4. RNA sequencing (RNA-seq) analysis

Fresh-frozen aortic samples for RNA-seq were obtained from independent cohorts of patients with similar clinical and demographic characteristics (Supplementary Table 1). Total RNA was extracted and evaluated for quality as described above. RNA-seq library preparation was performed using KAPA RNA HyperPrep Kits. All libraries were pooled and sequenced on 1 lane of a HiSeq 4000 instrument. The samples were sequenced to a mean depth of 30.86 million reads. FASTQC was utilized to inspect the raw sequencing data. Spliced Transcripts Alignment to a Reference (STAR, ver2.6) [19] was used to align the sequence reads to hg19, and RSEM (ver1.3.0) [20] was used to estimate the gene level abundance. Gene level count data were processed and normalized, and between-group analyses were performed in DESeq2 [21]. Weakly expressed genes with fewer than 80 counts in 50% of study samples were excluded from analysis. The remaining 8610 genes were subsequently utilized to identify DEGs between HSS and LSS groups. For validation of the genes identified from the discovery microarray analysis, the direction of effect was required to be consistent between the SS study groups, and the association levels were suitably adjusted for the number of multiple tests performed using a Bonferroni *p* value correction (Supplementary Fig. 2).

2.5. Human aortic tissue IL1B immunohistochemistry

A total of 8 independent human aortic tissues from the LSS and HSS

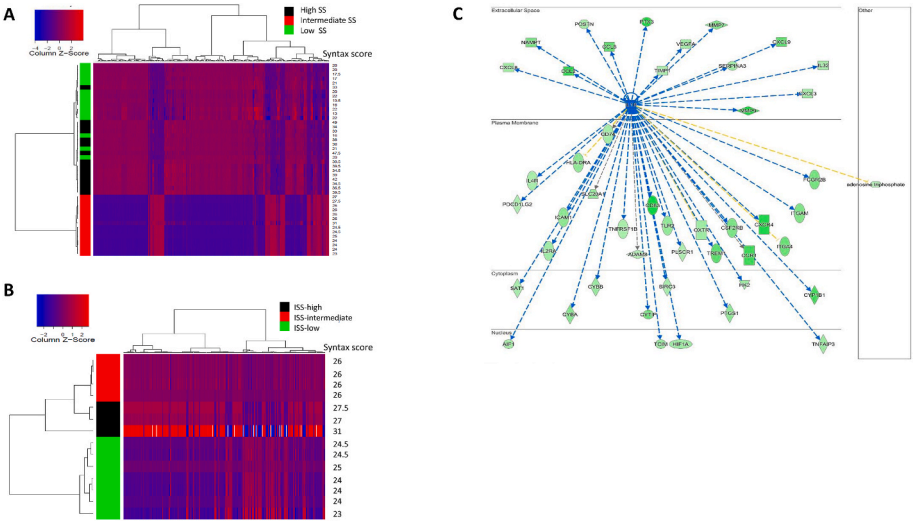

Fig. 2. Hierarchical clustering of SYNTAX score patient groups using the 432 DEGs identified in discovery analysis.
(A) Hierarchical clustering of HSS (High SS, SYNTAX >32, black), LSS (Low SS, SYNTAX <23, green) groups and ISS (Intermediate SS, SYNTAX between 23 and 32, red). (B) Clustering of the ISS group into ISS-high (SYNTAX ≥27.5, black), ISS-intermediate (SYNTAX between 24.5 and 27.5, red) and ISS-low (SYNTAX ≤24.5, green) groups. A total of 432 DEGs were identified in the discovery analysis. (C) Network of 47 genes connected with *IL1B* among the DEGs upregulated in LSS. The blue dashed line indicates the expected activation of genes, and the yellow dashed line indicates the expected inhibition of genes from all direct and indirect interactions of activation, expression, inhibition, transcription and protein-protein interactions, as curated from Ingenuity Pathway Analysis (IPA). The green shading represents the fold-change of the DEG identified in the study. (For interpretation of the references to colour in this figure legend, the reader is referred to the Web version of this article.)

groups were fixed using a formaldehyde fixation/paraffin embedding protocol. The patient characteristics were similar to those of other recruited patients (Supplementary Table 1). Aortic tissue punch samples were embedded and subsequently used to prepare histological slices that included the intimal, medial and adventitial layers of the arterial wall (Fig. 3A and B). Sections of 4-μm thickness were cut from the blocks for IL1B IHC. Each slide included at least 3 serial sections for analysis. Antigen retrieval was performed using a steamer in 0.01 M citrate buffer at pH 6.0 for 20 min. The tissue sections were incubated overnight with the IL1B primary antibody ab156791 (Abcam, UK) at a 1:50 dilution and then detected with a Dako EnVision + System K4001 (Agilent, CA, USA). Aortic tissues were counterstained with hematoxylin. IL1B IHC images were obtained under the same conditions with a Ni-E Ri2 microscope (Nikon, Japan) for the large brightfield images. Using QuPath 0.2.3 (open source software), we measured all parameters required for the total tissue area, stained area, total tissue cell number and stained cell number calculations based on methods established by previous studies [22,23]. Each graph shows the p value of Student's t-test, and $p < 0.05$ was considered statistically significant.

2.6. RNA-seq analysis of commercially obtained primary aortic VSMCs

To assess the transcript levels of VSMCs, we stimulated human VSMCs (PromoCell) with proinflammatory agents, creating conditions mimicking an atherosclerotic environment, *in vitro*. Cells in their third passage were used to conduct these experiments. The VSMCs were growth-arrested for 24 h in a serum-free environment and subsequently stimulated using a cocktail (IPCO) of inflammatory mediators (50 μg/ml oxidized low-density lipoprotein (oxLDL; Thermo Fisher Scientific, MA, USA), 10 ng/ml interleukin-1β (IL1-β; PeproTech, NJ, USA), 10 μM N^{ε}-carboxymethyllysine (CML; Cayman Chemicals, MI, USA), 10 ng/ml platelet-derived growth factor-BB (PDGF-BB; PeproTech, NJ, USA)) or further arrested over 48 h. Total RNA was extracted using TRIzol Reagent (Thermo Fisher Scientific, MA, USA) and a Direct-zol™ RNA MiniPrep Kit including DNase treatment using the manufacturer's protocol.

RNA quality and quantity were determined using a NanoVue Plus spectrophotometer (GE Healthcare) and an Agilent RNA 6000 Pico Kit (Agilent), which was run on an Agilent Technologies 2100 Bioanalyzer. Total RNA sequencing libraries were prepared using an Illumina TruSeq Stranded Total RNA Library Prep kit with Ribo-Zero Human/Mouse/Rat (Illumina, RS-122-2201) to deplete cytoplasmic rRNA according to the manufacturer's instructions. All cDNA libraries underwent QC using an Agilent DNA1000 Kit (Agilent) before next-generation sequencing. The samples were sequenced on an Illumina HiSeq 4000 to a depth of ~50 million paired-end reads per biological sample. The adaptors were trimmed using Trim Galore with the sequence parameter –length 50. The paired-end reads were mapped against the human reference genome GrCh38/hg38 using the STAR aligner with the default parameters. The gene counts were computed using htseq-count [24]. The gene counts were normalized to the counts per million (CPM), and differential gene expression (DE) analysis was performed using EdgeR [25]. Significant DEGs with a false discovery rate-adjusted p value < 0.05 and a logFC >0.5 were called. Figures were generated with R (Version 3.5.1) and GraphPad Prism (Version 7.0) (Fig. 4A and B).

2.7. Primary human VSMC isolation from the arterial walls of LSS and HSS patients

To isolate primary VSMCs, aortic tissues from the LSS or HSS groups were dissociated in an enzyme mix. In brief, tissue was collected in an operation theater and immediately stored in CUSTODIOL® HTK Solution (Essential Pharmaceuticals, NC, USA). Aortic tissues were rinsed in Dulbecco's phosphate-buffered saline (Thermo Fisher Scientific, MA, USA) and cut into 1 mm^3 pieces using a scalpel. The tissue pieces were then digested in enzyme mix solution containing collagenase type II (Sigma–Aldrich, MO, USA), elastase (Sigma–Aldrich, MO, USA), and DNase I (Sigma–Aldrich, MO, USA) for 2 h at 37 °C. The resulting cell suspension was filtered through a 100 μm sieve and washed with Hanks' Balanced Salt Solution (Thermo Fisher Scientific, MA, USA).

Primary VSMCs were subsequently cultured in SmGM™-2 Smooth Muscle Cell Growth Medium-2 BulletKit™ (Lonza Bioscience, Switzerland) in a humidified incubator with 5% CO_2 at 37 °C. The cells were subcultured every 5 days and seeded at a density of 3500 cells/cm^2. Cells from the third passage were used in the subsequent experiments. The identity of VSMCs was evaluated based on the expression of α-smooth muscle actin and von Willebrand factor following cell differentiation assessed by immunofluorescence (Fig. 5A).

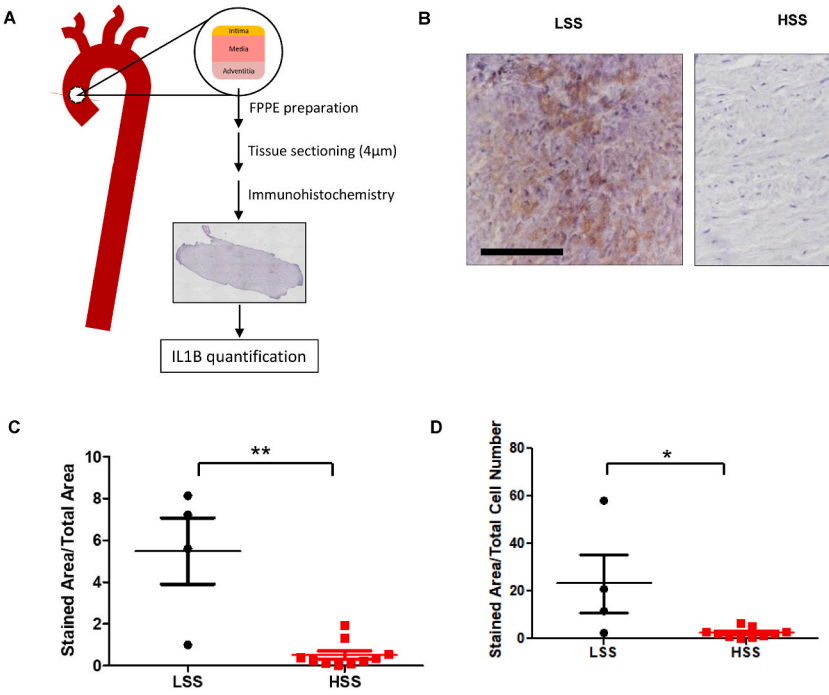

Fig. 3. Aortic tissues with low SYNTAX scores show strong expression of IL1B.
(A) Diagram showing the aortic wall tissue preparation for IL1B immunohistochemistry and quantification. (B) Immunohistochemical staining of IL1B in LSS and HSS human aortic tissue biopsy samples. The lower panels show magnified views of the insets in the upper panels. Scale bars, 100 μm. (C and D) Quantification of the stained area/total area and stained area/total cell number in IL1B immunohistochemistry. $^{**}p < 0.01$, $^{*}p < 0.05$.

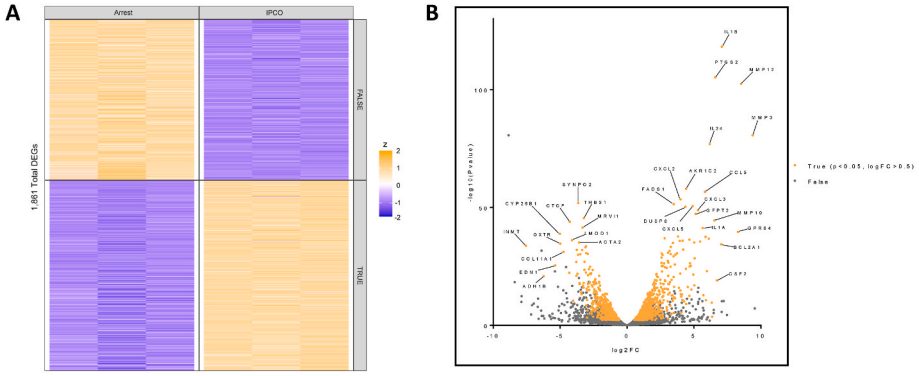

Fig. 4. RNA sequencing analysis of aortic smooth muscle cells stimulated for 48 h with a proatherogenic cocktail (IPCO; 10 ng/ml IL-1β + 10 ng/ml PDGF-BB + 10 μM CML + 50 μg/ml OxLDL) *vs.* nonstimulated arrested cells (arrest).
(A) Heatmap showing upregulated (orange) and downregulated (blue) DEGs after growth arrest and IPCO treatment. (B) Volcano plot depicting 1861 DEGs as orange dots as defined by a false discovery rate-adjusted p value < 0.05 and logFC >0.5. (For interpretation of the references to colour in this figure legend, the reader is referred to the Web version of this article.)

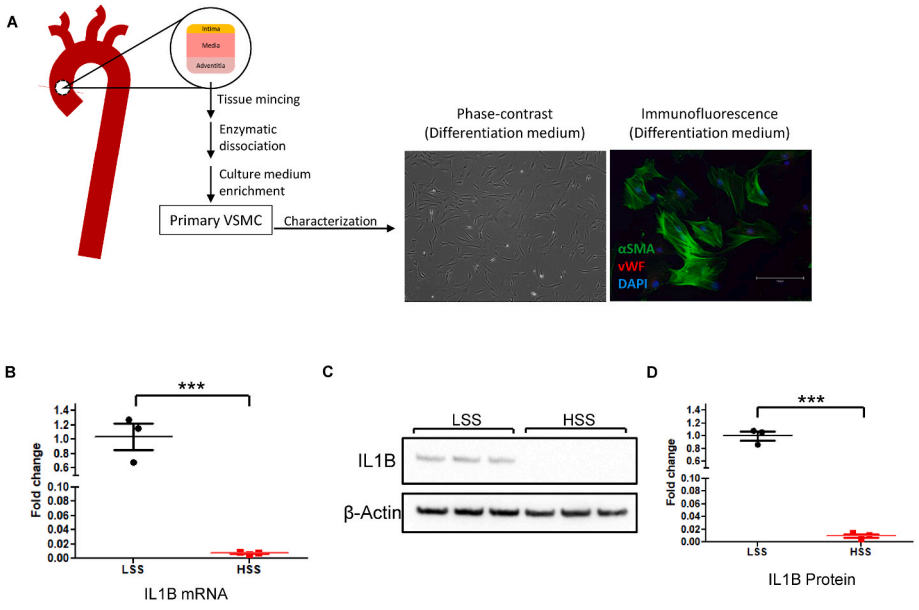

Fig. 5. Primary VSMCs derived from LSS aortic tissue express high levels of IL1B mRNA and protein.
(A) Diagram showing primary VSMC isolation from aortic tissue via enzymatic dissociation. Primary VSMCs were characterized by α-SMA and vWF immunofluorescence after 24 h of differentiation. (B) *IL1B* mRNA expression levels in primary VSMCs derived from LSS and HSS human aortic tissues as measured by RT-qPCR analysis. The values presented in the chart were obtained from three independent repeats. ***$p < 0.005$. (C) Immunoblotting of IL1B protein in primary VSMCs derived from LSS and HSS human aortic tissues. (D) Quantification of IL1B protein levels in primary VSMCs derived from LSS and HSS human aortic tissues normalized to β-actin levels. The values presented in the chart were obtained from three independent repeats. ***$p < 0.005$.

2.8. *IL1B reverse transcription–quantitative polymerase chain reaction*

Total RNA from primary human VSMCs was isolated with an E.Z.N.A.® Total RNA Kit I (Omega Bio-Tek, GA, USA) according to the manufacturer's protocol. Total RNA concentration and quality were evaluated as described above. Total cDNA was prepared with All-In-One 5X RT MasterMix (Applied Biological Materials, Canada) according to the manufacturer's protocol. The expression levels of *IL1B* (Forward 5′-CCACAGACCTTCCAGGAGAATG-3'; Reverse 5′-GTGCAGTTCAGTGATCGTACAGG-3′) and the housekeeping gene *GAPDH* (Forward: 5′-TGACCTCAACTACATGGTTTACA-3'; Reverse: 5′-TCGCCCCACTTGATTTTGGA-3′) were measured by RT–qPCR using TETRA™ 2X qRT–PCR master mix (Youseq, UK) via a LineGene 9620 Real Time-PCR Detection System (Bioer, China). For each sample, the *IL1B* gene expression level was normalized to the corresponding *GAPDH* expression level and analyzed using the $2^{-\Delta\Delta CT}$ method. Statistical significance was calculated using Student's *t*-test, and a value of $p < 0.05$ was considered to indicate statistical significance.

2.9. *IL1B immunoblotting*

Total protein from primary VSMCs was collected using T-PER™ Tissue Protein Extraction Reagent (Thermo Fisher Scientific, MA, USA) supplemented with Halt™ Protease Inhibitor Cocktail (Thermo Fisher Scientific, MA, USA). The total protein concentration was determined using a Pierce™ Rapid Gold BCA Protein Assay Kit (Thermo Fisher Scientific, MA, USA). For immunoblotting, total protein was separated with an Invitrogen NuPAGE™ 4–12%, Bis-Tris gel electrophoresis system (Thermo Fisher Scientific, MA, USA). The extracted proteins were transferred to PVDF membranes and incubated with primary and secondary antibodies. IL1B immunoblotting was performed using the IL1B antibody ab9722 (Abcam, UK) at a 1:1000 dilution and the secondary goat anti-rabbit HRP-conjugated antibody G21234 (Thermo Fisher Scientific, MA, USA) at a 1:100,000 dilution. The membrane was immunoblotted with the HRP-conjugated β-actin antibody sc-47778 (Santa Cruz Biotechnology, TX, USA) as loading control. Immunoblot images were obtained with an iBright 1500 Imaging System (Thermo Fisher Scientific, MA, USA) and analyzed with iBright Analysis Software (Thermo Fisher Scientific, MA, USA). The IL1B protein level was normalized to the β-actin level. Statistical significance was calculated using Student's *t*-test, and a value of $p < 0.05$ was considered to indicate statistical significance.

2.10. *In vivo mouse atherosclerosis model*

Female *Apoe*$^{-/-}$ mice (approximately 18 g) were purchased from Jackson Laboratory (Bar Harbor, ME). All animal experiments were performed according to the guidelines of the Institutional Animal Care and Use Committee (National University of Singapore, Singapore) and were approved by the local ethics committee. The mice were maintained

on a high-fat diet (21% fat and 0.15% cholesterol; Herlan Teklad, WI) from 6 weeks of age according to the IACUC R18-0080 protocol which been described in the literature [26]. The animals were divided into two groups: an early atherosclerosis group (10 weeks of age, 4 weeks on the high-fat diet) and a late atherosclerosis group (24 weeks of age, 18 weeks on the high-fat diet) [27,28].

Mouse arterial wall IHC was performed after the *Apoe*$^{-/-}$ mice were sacrificed and their aortas were harvested and frozen instantly in Tissue-Tek Optimum Cutting Temperature compound (Tissue-Tek OCT, Sakura Finetek, USA) for 10 μm cryosectioning. For this experiment, the proximal parts of the mouse ascending aorta were used, which anatomically correlate to the area of the human aorta where the aortic punches were collected (Fig. 6A). For the early and late disease models, at least 2 slides per mouse were used to perform staining. Each slide included at least 3 serial sections. The tissue sections were first fixed in ice-cold acetone for 10 min, incubated with 0.2% BSA blocking solution and then stained with antibodies for 2 h at room temperature. The primary antibodies used included a rabbit anti-mouse IL1B antibody (Abcam; ab205924) at a 1:500 dilution and a rat anti-mouse CD68 antibody (identifies macrophages; Bio–Rad, MCA1967) at a 1:300 dilution. Cy3-or Alexa Fluor 488-conjugated anti-rabbit, anti-rat and anti-Armenian hamster antibodies (Jackson ImmunoResearch Laboratories) were used for detection. The sections were counterstained with 4,6-diamidino-2-phenylindole (DAPI) for cell nucleus visualization and mounted with fluorescent mounting medium for analysis. The specimens were viewed with a fluorescence wide field (Axio Imager.Z1, AxioCam HRm camera; Carl Zeiss Micro Imaging, Jena, Germany). The total valve area and sum intensity of IL1B and CD68 were measured using QuPath 0.2.3 (open source software). IL1B and CD68 expression was calculated as the fold change of the sum intensity/total valve area and analyzed using Student's *t*-test, where a p value < 0.05 was considered to indicate statistical significance. For lipid staining, aortic sections were stained with hematoxylin and oil red O and visualized using a brightfield microscope.

3. Results

3.1. Low-SYNTAX-score patients have elevated expression of IL1B in aortic wall tissue

We identified a total of 432 significant DEGs between the HSS and LSS groups in our discovery gene expression analysis ($p_{Adj} < 0.05$ and FC > 1.5) (Supplementary Table 2). A total of 173 genes were upregulated in the LSS group, while 259 genes were upregulated in the HSS group. Hierarchical clustering using these 432 DEGs separated the LSS, ISS and HSS samples, with 1 HSS subject and 3 LSS subjects misclassified (Fig. 2A). Additional hierarchical analysis with set of ISS samples clustering to HSS and LSS revealed a clear separation between three groups of patients (Fig. 2B).

To evaluate whether the identified DEGs had prior relevance to CAD, we overlapped these hits with genes involved with CAD from the GeneCards database (https://www.genecards.org/). A significant number of identified DEGs overlapped with prior CAD-related genes from GeneCards (214 out of 432 genes, binomial $p = 0.0376$) (Supplementary Table 2), indicating the overall relevance of the identified hits to CAD.

Pathway-based analysis using the 432 DEGs showed significant enrichment in 136 pathways ($p_{Adj} < 0.05$, Supplementary Table 3). The majority of these pathways presented significantly enriched DEGs upregulated in LSS patients and included atherosclerosis signaling pathways, several immune pathways and inflammation-associated pathways involving the genes *IL1B*, *APOC1*, *CCL2*, *CXCL8*, *CXCR4*, *ICAM1*, *ITGA4*, *ITGB2*, *MMP9*, *PCYOX1*, *PDGFC*, and *RBP4* (Supplementary Fig. 2 and Supplementary Table 4). The significant pathway terms that were enriched only among DEGs upregulated in HSS patients were largely reflective of cell/tissue remodeling and cardiogenesis processes, such as factors promoting cardiogenesis in vertebrates, tight junction signaling, regulation of actin-based motility by rho, gap junction and actin cytoskeleton signaling pathways (Supplementary Fig. 2 and Supplementary Table 5).

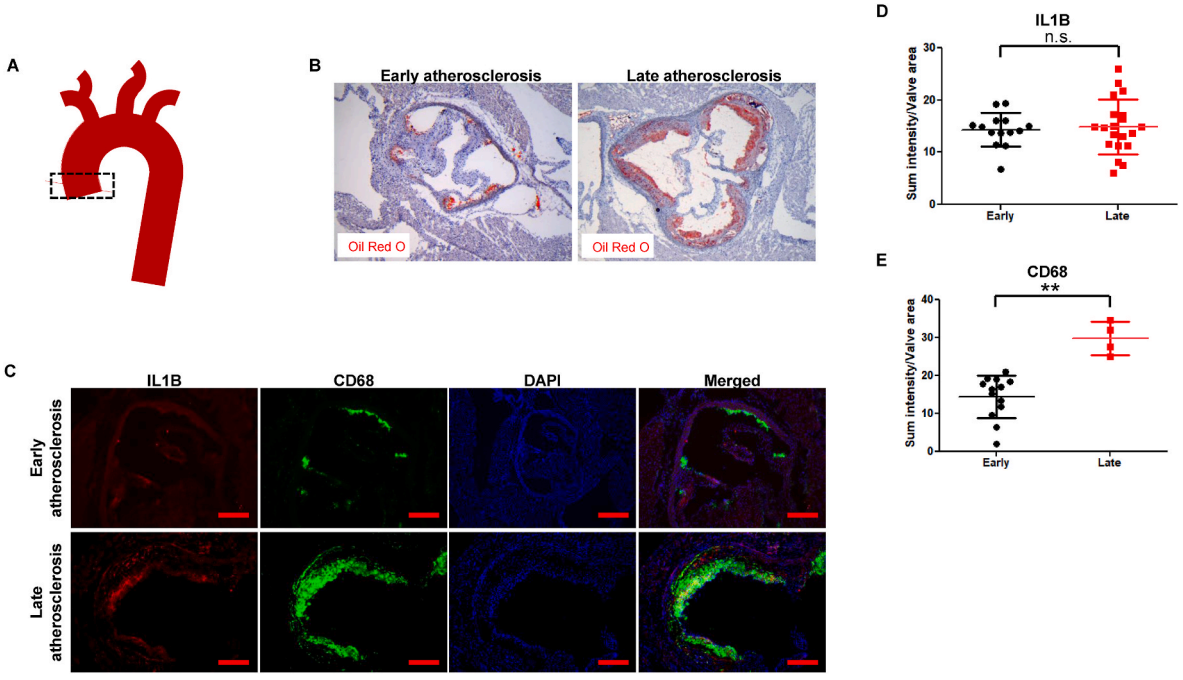

Fig. 6. IL1B expression is not dependent on the stage of atherosclerosis in an *in vivo* mouse model of atherosclerosis.
(A) Diagram showing the location of the Apoe$^{-/-}$ mouse aortic root tissue for Oil Red O, IL1B, and CD68 staining. (B) Oil Red O staining of aortic root tissue of *Apoe*$^{-/-}$ mice with early and late atherosclerosis. (C) Immunofluorescence staining of IL1B and CD68 in aortic root tissue of *Apoe*$^{-/-}$ mice with early and late atherosclerosis. Scale bar, 200 μm. (D and E) Quantification of the total intensity/valve area of IL1B and CD68 immunofluorescence in aortic root tissue of *Apoe*$^{-/-}$ mice with early and late atherosclerosis. $^{**}p < 0.01$. (For interpretation of the references to colour in this figure legend, the reader is referred to the Web version of this article.)

Upstream regulator evaluation using the 173 DEGs with elevated expression in LSS patients indicated *IL1B* as the top upstream regulator also identified as a significant DEG in the study (Supplementary Table 6). The network analysis with the *IL1B* hub gene indicated an interconnected set of 47 genes within the LSS patient group (Fig. 2C). In contrast, significant regulators identified using upregulated genes in the HSS patients did not overlap with any DEGs identified in the study (Supplementary Table 7).

We further validated the expression of *IL1B* and *IL1B*-connected genes in an independent RNA-seq dataset of HSS and LSS patients. *IL1B* and *FCGR2B* were observed to have the strongest associations and increased expression among the LSS patients in the replication set (compared to HSS patients, P_{Adj} between 0.013 and 7.52×10^{-3}), while 12 other *IL1B*-connected genes were nominally associated and had consistently increased expression among the additional LSS patients (p between 0.044 and 2.04×10^{-3}, binomial $p = 1.30 \times 10^{-7}$) (Table 1). Overall, the gene expression patterns of the identified DEGs from discovery analysis were highly consistent in the RNA-seq dataset, with at least 118 DEGs showing nominal associations (p between 0.049 and 1.33×10^{-7}) with consistent direction of effects (binomial $p < 0.00001$) (Supplementary Table 2).

3.2. The IL1B protein was upregulated in LSS aortic tissues compared to HSS aortic tissues

We evaluated the presence of the IL1B protein in LSS and HSS aortic tissues using IHC (Fig. 3A and B). The stained samples underwent quantification analysis using two parameters. Based on the quantifications of stained area/total area (Fig. 3C) and stained area/total cell number (Fig. 3D), IL1B expression in LSS aortic tissues was elevated by 10.56-fold ($p = 0.0167$) and 9.4-fold ($p = 0.0003$), respectively, in comparison to that in HSS aortic tissues.

3.3. Stimulated VSMCs revealed that IL1B expression was increased in atherosclerotic conditions

In vitro stimulation of VSMCs revealed 1861 DEGs in stimulated VSMCs compared to unstimulated VSMCs, FDR <0.05 and logFC >0.5 (Supplementary Table 8). Hierarchical clustering analysis revealed clear separation between stimulated and unstimulated groups (Fig. 4A). Pathway analysis of DEGs revealed upregulation of inflammatory and immune related processes in stimulated VSMCs (Supplementary Figs. 3A–C). *IL1B* was observed to be the most significantly upregulated gene when VSMCs were stimulated in atherosclerotic conditions (logFC = 7.083, $FDR = 1.38 \times 10^{-114}$) (Fig. 4B and Supplementary Table 8). Fifteen other genes identified to be connected to *IL1B* in our network analysis, namely, *NAMPT*, *SAT1*, *CXCR4*, *TNFRSF1B*, *TNFAIP3*, *ICAM1*, *HK2*, *SLC20A1*, *TREM1*, *IL32*, *BIRC3, PTX3, CCR1, CYP1B1* and *CCL8*, were also consistently upregulated in stimulated VSMCs compared to unstimulated VSMCs (*FDR* between 0.015 and 3.73×10^{-30}, Supplementary Table 8). Overall, we observed a significant enrichment of *IL1B* and *IL1B*-related genes that were identified to be upregulated in LSS aortic tissues and were also consistently upregulated among the stimulated VSMCs (binomial $p < 0.00001$).

Table 1
Summary of the association results for IL1B and the differentially expressed genes (DEGs) identified to be connected to IL1B in the discovery and replication datasets.

		Discovery microarray			Replication RNAseq		
		15 HSS vs 15 LSS			3 HSS vs 3 LSS		
Gene	Gene name	LgFC	p	p_{Adj}	LgFC	p	p_{Adj}
FCGR2B	Fc fragment of IgG receptor IIb	−0.973	1.98E-03	0.015	−3.713	2.03E-04	7.52E-03
IL1B	interleukin 1 beta	−0.993	2.28E-05	1.14E-03	−5.083	3.54E-04	0.013
ADAM8	ADAM metallopeptidase domain 8	−0.599	1.48E-05	9.51E-04	−3.099	2.04E-03	0.075
NAMPT	nicotinamide phosphoribosyltransferase	−0.976	2.92E-06	5.15E-04	−2.169	2.05E-03	0.076
CCR1	C–C motif chemokine receptor 1	−1.310	2.00E-05	1.09E-03	−4.624	2.07E-03	0.077
TIMP1	TIMP metallopeptidase inhibitor 1	−0.622	4.51E-03	0.024	−2.208	2.30E-03	0.085
CYBA	cytochrome *b*-245 alpha chain	−0.841	7.88E-04	8.43E-03	−1.585	3.34E-03	0.123
IL2RA	interleukin 2 receptor subunit alpha	−0.664	5.78E-03	0.029	−4.642	5.89E-03	0.218
PTGS1	prostaglandin-endoperoxide synthase 1	−0.816	9.28E-04	9.21E-03	−2.969	0.007	0.269
CD74	CD74 molecule	−0.660	0.011	0.046	−1.329	0.011	0.399
SAT1	spermidine/spermine N1-acetyltransferase 1	−0.644	7.13E-04	7.98E-03	−1.569	0.012	0.441
HLA-DRA	major histocompatibility complex, class II, DR alpha	−0.801	4.73E-03	0.025	−1.249	0.030	1
POSTN	periostin	−0.705	7.69E-03	0.035	−1.574	0.043	1
AIF1	allograft inflammatory factor 1	−0.672	4.20E-03	0.023	−1.105	0.044	1
TLR2	toll like receptor 2	−0.773	1.12E-03	0.010	−1.921	0.052	1
TREM1	triggering receptor expressed on myeloid cells 1	−1.125	1.73E-03	0.014	−2.369	0.058	1
IL32	interleukin 32	−0.674	9.67E-04	9.42E-03	−1.346	0.061	1
HK2	hexokinase 2	−0.741	1.43E-06	3.91E-04	−2.243	0.063	1
CCL8	C–C motif chemokine ligand 8	−1.126	5.76E-03	0.029	−1.492	0.116	1
CYBB	cytochrome *b*-245 beta chain	−0.743	0.012	0.048	−1.733	0.157	1
BIRC3	baculoviral IAP repeat containing 3	−0.636	1.98E-04	3.66E-03	−1.394	0.181	1
CD83	CD83 molecule	−1.512	7.42E-08	1.38E-04	−1.347	0.242	1
ITGAM	integrin subunit alpha M	−0.911	6.81E-03	0.032	−1.185	0.247	1
SLC20A1	solute carrier family 20 member 1	−0.789	6.17E-06	6.84E-04	1.205	0.288	1
HIF1A	hypoxia inducible factor 1 subunit alpha	−0.718	1.01E-04	2.45E-03	−0.910	0.360	1
CYTIP	cytohesin 1 interacting protein	−1.021	1.93E-04	3.62E-03	−1.245	0.391	1
TNFAIP3	TNF alpha induced protein 3	−0.707	3.67E-04	5.31E-03	1.072	0.398	1
CXCR4	C-X-C motif chemokine receptor 4	−1.445	2.82E-04	4.51E-03	−1.049	0.410	1
IL4R	interleukin 4 receptor	−0.620	2.91E-05	1.28E-03	0.789	0.520	1
MMP9	matrix metallopeptidase 9	−1.569	5.77E-04	6.86E-03	−0.567	0.581	1
TNFRSF1B	TNF receptor superfamily member 1B	−0.635	9.63E-04	9.40E-03	0.557	0.612	1
CYP1B1	cytochrome P450 family 1 subfamily B member 1	−1.280	6.94E-04	7.85E-03	−1.115	0.637	1
CXCL9	C-X-C motif chemokine ligand 9	−1.160	4.55E-04	5.95E-03	−0.510	0.687	1
ICAM1	intercellular adhesion molecule 1	−0.811	3.78E-05	1.48E-03	0.328	0.726	1
PTX3	pentraxin 3	−1.499	1.57E-05	9.71E-04	−0.193	0.913	1
PLSCR1	phospholipid scramblase 1	−0.596	4.27E-04	5.71E-03	−0.066	0.924	1
CCL2	C–C motif chemokine ligand 2	−1.424	2.01E-05	1.09E-03	−0.039	0.961	1

3.4. IL1B was upregulated in primary VSMCs derived from LSS aortic tissues

To further validate the expression of IL1B in the LSS and HSS groups, primary VSMCs were isolated from patients' aortic tissues (Fig. 5A). Consistent with the gene expression data, primary VSMCs from the LSS group showed 143-fold higher *IL1B* mRNA levels than those from the HSS group ($p = 0.0048$) (Fig. 5B). Similarly, based on immunoblot analysis, we found that primary VSMCs from the LSS group expressed 102-fold higher IL1B protein levels than those from the HSS group ($p = 0.0002$) (Fig. 5C and D).

3.5. Mouse IL1B staining based on disease progression

The effectiveness of establishment of the apolipoprotein E-deficient (*apoe*$^{-/-}$) mouse model, a well-established atherosclerosis mouse model, was confirmed by Oil Red O and CD68 staining (Fig. 6A and B). The staining revealed progressive lipid and macrophage accumulation in the mouse arterial wall based on the early and late stages of atherosclerotic disease. As the disease progressed from an early stage (10-week-old *apoE*$^{-/-}$ mice) to a more advanced stage (24-week-old *apoE*$^{-/-}$ mice), we noted an increase in lipids and necrotic core formation within the arterial wall (Fig. 6C and E). After establishing disease progression, we analyzed the presence and distribution of IL1B in the arterial wall. IL1B expression predominantly accumulated within the atherosclerotic plaques of the arterial wall. Notably, IL1B was observed in early and late disease, with a trend toward increased expression in later disease; however, quantification did not present a significant difference (Fig. 6D).

4. Discussion

In basic research, the ultimate goal is to identify a pathophysiological process that can be targeted in clinical practice. Millions of cardiovascular deaths related to atherosclerosis are reported every year despite advances in medical therapy, indicating that understanding of atherosclerosis in coronary arteries is far from being achieved. Even with optimal modern therapy, recurrent cardiovascular events are documented in up to 14.3% of specific populations [29].

Although low-density lipoprotein cholesterol (LDL-C) reduction strategies remain a cornerstone in CAD prevention and management, a large proportion of patients may not achieve an optimal clinical response even with statin treatment and an optimized lipid profile [30]. Moreover, varied effects are observed in relation to coexisting cardiometabolic diseases such as obesity and diabetes [5,31].

In addition to dyslipidemia and metabolic disfunctions, inflammation of the arterial wall is an important hallmark of CAD, and mitigation of inflammatory processes represents an unmet therapeutic need in CAD [32]. The practical application of anti-inflammatory therapy is, however, complicated by several factors and only few of these therapies progress to clinical studies. There are several reasons for this delay. Firstly, understanding of inflammation in atherosclerosis is rather controversial [33]. This is especially true for cytokines engagement in inflammation, as their involvement is often multifactorial, and few bidirectional effects have been reported. The second factor, which complicates application of anti-inflammatory therapy, is related to the fact that the majority of experimental work has been done using nonhuman tissue or animal models [34]. There are many examples of promising results in animal models, with controversial or minimal effects in clinical trials [35]. IL1B, for example, has been extensively shown to be related to atherosclerosis in a mouse model [36]. A recent study on the *Apoe*$^{-/-}$ *Myh11* Cre ER^{T2} R26R–YFP mouse model showed that the IL1B effect might vary at different stages of the pathophysiological process and that in the advanced stage of plaque development, IL1B may have an opposite atheroprotective effect [36].

Based on this understanding, appropriate patient subpopulations that may benefit from IL1B therapy have yet to be identified. The Canakinumab Anti-inflammatory Thrombosis Outcome Study (CANTOS) was the first large-scale clinical study to show that anti-inflammatory treatment with canakinumab, a monoclonal antibody targeting IL1B, reduces cardiovascular complications independently of reductions in lipid levels [3,37,38]. The CANTOS trial, however, showed only a 15% reduction in the primary endpoint with an IL1B antibody (canakinumab) in a phase III human clinical trial [5,31,32]. Nevertheless, it is important to highlight that participants in the CANTOS trial with high levels of inflammation defined by baseline levels of high-sensitivity C-reactive protein (hsCRP), benefited the most from anti-inflammatory interventions compared to those with a lower inflammatory marker. Another trial, the Cardiovascular Inflammation Reduction Trial (CIRT), which did not select cardiovascular disease participants on the basis of elevated systemic inflammation, did not show cardiovascular benefit [39]. These findings suggest that sub-groups of individuals with inflammatory dysfunctions may benefit more from such anti-inflammatory interventions for CAD.

Sirolimus, also known as rapamycin, is another example of an effective immunosuppressant application to address vessel wall cell proliferation and preventing restenosis in CAD. Of interest, application of drug-eluting stents (DESs) loaded with rapamycin in percutaneous coronary intervention was more effective in patients with low-SS. This emphasizes the potential discriminative power of SS in identifying appropriate patient groups that may benefit most from such intervention [40]. It proves again that SS is a well-validated clinical tool providing patient-specific clinical strategies, useful for differential management [41].

We used the SYNTAX score to divide clinical groups into a low-SYNTAX-score group (with fewer lesions in coronary arteries), and intermediate-SYNTAX-score group, and a high-SYNTAX-score group (with multiple and frequently diffuse coronary lesions). We believe that our study is the first to evaluated human arteries transcript in association with the complexity of atherosclerotic lesions in coronary disease. Tissue transcriptomic data were obtained from arterial biopsies and stratified based on the SS scale: low, intermediate, and high. The result showed that DEGs between these groups were enriched in pathways, related to immune response and inflammation and include *IL1B*, *APOC1*, *CCL2*, *CXCL8*, *CXCR4*, *ICAM1*, *ITGA4*, *ITGB2*, *MMP9*, *PCYOX1*, *PDGFC*, and *RBP4* genes. Among the three groups, the LSS group exhibited significant upregulation of identified immune and inflammatory pathways. Our data revealed that in the LSS group, IL1B was the top upstream regulator directly connected with the vast majority of DEGs. This data clearly identified IL1B as a key inflammatory molecule in the arterial tissue among patients with low-SS. This genetic data was validated in an independent cohort of patient's samples using NGS. The presence of the IL1B protein in tissue was confirmed with quantitative IHC obtained from HSS and LSS groups. As LSS tissue expresses higher level of proinflammatory transcript, it would indirectly provide a plausible explanation of why treatment of LSS patients with DESs, which utilizes sirolimus and its local anti-inflammatory properties, might be more effective [42].

Previously published works demonstrated conflicting correlations between inflammatory markers and SS that may be confounded by the presence of other CAD risk factors [43–45]. Our well-matched (lipid levels and other CAD risk factors) samples with different SS may have enabled us for a more precise identification of inflammatory dysfunctions in CAD patients. Additionally, most studies have evaluated inflammatory marker levels in plasma, which may imprecisely reflect on inflammatory dysfunctions at primary disease-relevant tissue – arteries and may, in part, account for our study findings.

The presence of IL1B signaling in the arterial wall drove our interest in its origin at the cellular level. As IHC staining for IL1B revealed strong signal in media, our attention focused on VSMCs. VSMCs are one of the most abundant cell types in vessel wall media. Newer technologies, including *in situ* hybridization assays, single-cell sequencing technology,

and *in vivo* fate tracing using the CreER^{T2}-loxP system, have deepened our knowledge of these dynamic and interesting cells [46]. The contractile and synthetic VSMC phenotypes have been known for a long time and have been expanded to include VSMC macrophage-like cells that are heavily involved in vessel wall inflammation. It is now known that VSMC plasticity and the ability to perform nonprofessional phagocytic functions play a key role in maintaining the inflammatory state [47]. To prove that VSMCs could be a potential source of IL1B, we used VSMCs culture. Our RNA-seq analysis in VSMCs stimulated with the proinflammatory cocktail IPCO, revealed a marked upregulation of *IL1B*. To address the limitations of commercial primary cells, we specifically isolated primary VSMCs in arterial biopsies from LSS and HSS patients for further experimental work. The comparative results confirmed that VSMCs from patients with LSS exhibited upregulated levels of *IL1B* gene expression and genetic data translated to elevated IL1B protein.

These ambiguous results that LSS patients had proinflammatory tissue phenotype, raised another question: do SYNTAX scores represent stages of disease progression, or do they reveal the different patterns of coronary disease distinguished by different pathological backgrounds of specific patients? To evaluate the levels of IL1B in the different stages of atherosclerosis, we utilized the well-established *apoe*$^{-/-}$ mouse model and a high-fat diet. We were able to see the progression of atherosclerosis based on Oil Red O staining and the presence of CD68-positive cell differences in the early and late stages of the disease. Our mouse model comparing the early and late stages of the disease revealed a trend toward higher levels of IL1B ($p > 0.05$) and CD68 in the late stage of disease model (female *apoe*$^{-/-}$ mice, high-fat diet). This data from the mouse model confirm that atherosclerosis progression correlates with increased inflammatory processes.

If we assume that the SYNTAX score also represents the stage of disease (i.e., more lesions drive the score higher such that a higher score indicates a later stage of the disease), it is expected that a higher score is associated with higher levels of inflammatory processes. However, in our transcriptomic, proteomic and cell culture analyses, the results showed that the LSS group presented upregulation of ILB gene expression in relation to inflammatory processes. These data prompted us to look at the SYNTAX score as a pattern representing differences at pathophysiological level. Notably, patients with specific risk factors, such as diabetes mellitus or smoking history, have more diffuse lesions on the coronary tree (hence, a higher SS). A few studies have revealed that patients with different SYNTAX scores also have different histological characteristics in the arterial wall [48,49].

Some limitations of this study should be considered. One is the absence of direct tissue specimens from coronary arteries and the use of ascending aortic tissues in the experiments instead. Even though the embryological origins of coronary arteries and aortic roots are very similar, the data still have to be interpreted with caution. Another limitation is the modest sample size because of the limited availability of human arterial tissue.

Overall, our study shows that IL1B expression in the arterial wall correlates with the LSS pattern of CAD. The effectiveness of DESs in patients with LSS may be an indirect evidence supporting this discovery. Moreover, based on our study, we believe that LSS patients with elevated levels of IL1B represent a specific group in which inflammation could play a substantial role in disease pathogenesis. Based on the upregulation of inflammatory processes, a low SYNTAX score is unlikely to represent a stage of disease progression but rather a specific pattern associated with certain pathophysiological processes. All together, these findings suggest that the LSS group is a plausible cohort of patients for whom anti-inflammatory therapy could be considered.

Financial support

This work was supported by National University of Singapore Start-up Grant (NUHSRO/2014/063/SU/01), National University Health System Bridging Funds (NUHSRO/2017/023/Bridging/05), Ministry of Education Academic Research Fund Tier 1 (T1-NUHS Joint Grant Call FY17-2nd call-13) and Lee Foundation Singapore (Single Cell Microfluidic Platform for Cardiovascular Disease).

CRediT authorship contribution statement

Rajkumar Dorajoo: Conceptualization, Methodology, Validation, Formal analysis, Investigation, Resources, Data curation, Writing – original draft, Writing – review & editing, Visualization, Funding acquisition. **Mario Octavianus Ihsan:** Conceptualization, Methodology, Validation, Formal analysis, Investigation, Data curation, Writing – original draft, Writing – review & editing, Visualization. **Wenting Liu:** Validation, Formal analysis, Resources, Data curation, Writing – original draft, Writing – review & editing, Visualization. **Hwee Ying Lim:** Validation, Formal analysis, Investigation, Resources, Data curation, Writing – original draft, Writing – review & editing, Visualization. **Veronique Angeli:** Validation, Formal analysis, Investigation, Resources, Data curation, Writing – original draft, Writing – review & editing, Visualization. **Sung-Jin Park:** Validation, Formal analysis, Investigation, Resources, Data curation, Writing – original draft, Writing – review & editing, Visualization. **Joyce M.S. Chan:** Validation, Formal analysis, Investigation, Resources, Data curation, Writing – original draft, Writing – review & editing, Visualization. **Xiao Yun Lin:** Writing – review & editing, Visualization, Project administration. **Mei Shan Ong:** Investigation, Writing – review & editing. **Umamaheswari Muniasamy:** Investigation, Writing – review & editing. **Chi-Hang Lee:** Conceptualization, Writing – review & editing. **Rijan Gurung:** Conceptualization, Investigation, Writing – review & editing. **Hee Hwa Ho:** Conceptualization, Writing – review & editing. **Roger Foo:** Conceptualization, Resources, Writing – review & editing. **Jianjun Liu:** Conceptualization, Resources, Writing – review & editing. **Theo Kofidis:** Conceptualization, Resources, Writing – review & editing. **Chuen Neng Lee:** Conceptualization, Resources, Writing – review & editing. **Vitaly A. Sorokin:** Conceptualization, Methodology, Validation, Formal analysis, Investigation, Resources, Data curation, Writing – original draft, Writing – review & editing, Visualization, Supervision, Project administration, Funding acquisition.

Declaration of competing interest

The authors declare that they have no known competing financial interests or personal relationships that could have appeared to influence the work reported in this paper.

Appendix A. Supplementary data

Supplementary data to this article can be found online at https://doi.org/10.1016/j.atherosclerosis.2022.12.005.

References

[1] J. Erdmann, T. Kessler, L. Munoz Venegas, H. Schunkert, A decade of genome-wide association studies for coronary artery disease: the challenges ahead, Cardiovasc. Res. 114 (2018) 1241–1257, https://doi.org/10.1093/cvr/cvy084.
[2] A.W. Turner, D. Wong, C.N. Dreisbach, C.L. Miller, GWAS reveal targets in vessel wall pathways to treat coronary artery disease, Front. Cardiovasc. Med. 5 (2018) 72, https://doi.org/10.3389/fcvm.2018.00072.
[3] P. Libby, Interleukin-1 beta as a target for atherosclerosis therapy: biological basis of CANTOS and beyond, J. Am. Coll. Cardiol. 70 (2017) 2278–2289, https://doi.org/10.1016/j.jacc.2017.09.028.
[4] W. Mai, Y. Liao, Targeting IL-1β in the treatment of atherosclerosis, Front. Immunol. 11 (2020), 589654, https://doi.org/10.3389/fimmu.2020.589654.
[5] K.C. Maki, P.M. Ridker, W.V. Brown, S.M. Grundy, N. Sattar, The diabetes subpanel of the national lipid association expert panel, an assessment by the statin diabetes safety task force: 2014 update, J.Clin. Lipidol. 8 (2014) S17–S29, https://doi.org/10.1016/j.jacl.2014.02.012.
[6] J. Lee, J.M. Ahn, J.H. Kim, et al., Prognostic effect of the SYNTAX Score on 10-year outcomes after left main coronary artery revascularization in a randomized

population: insights from the extended PRECOMBAT trial, J. Am. Heart Assoc. 10 (2021), e020359, https://doi.org/10.1161/JAHA.120.020359.
[7] R. Joehanes, S. Ying, T. Huan, et al., Gene expression signatures of coronary heart disease, Arterioscler. Thromb. Vasc. Biol. 33 (2013) 1418–1426, https://doi.org/10.1161/ATVBAHA.112.301169.
[8] C. Taurino, W.H. Miller, M.W. McBride, et al., Gene expression profiling in whole blood of patients with coronary artery disease, Clin. Sci. 119 (2010) 335–343, https://doi.org/10.1042/CS20100043.
[9] J.A. Wingrove, S.E. Daniels, A.J. Sehnert, et al., Correlation of peripheral-blood gene expression with the extent of coronary artery stenosis, Circ.Cardiovasc. Genet. 1 (2008) 31–38, https://doi.org/10.1161/CIRCGENETICS.108.782730.
[10] M.R. Elashoff, J.A. Wingrove, P. Beineke, et al., Development of a blood-based gene expression algorithm for assessment of obstructive coronary artery disease in non-diabetic patients, BMC Med. Genom. 4 (2011) 26, https://doi.org/10.1186/1755-8794-4-26.
[11] M. Pjanic, C.L. Miller, R. Wirka, J.B. Kim, D.M. DiRenzo, T. Quertermous, Genetics and genomics of coronary artery disease, Curr. Cardiol. Rep. 18 (2016) 102, https://doi.org/10.1007/s11886-016-0777-y.
[12] B. Liu, M. Pjanic, T. Wang, et al., Genetic regulatory mechanisms of smooth muscle cells map to coronary artery disease risk loci, Am. J. Hum. Genet. 103 (2018) 377–388, https://doi.org/10.1016/j.ajhg.2018.08.001.
[13] A.A. Derda, C. C Woo, T. Wongsurawat, et al., Gene expression profile analysis of aortic vascular smooth muscle cells reveals upregulation of cadherin genes in myocardial infarction patients, Physiol. Genom. 50 (2018) 648–657, https://doi.org/10.1152/physiolgenomics.00042.2017.
[14] R.A. Irizarry, B.M. Bolstad, F. Collin, L.M. Cope, B. Hobbs, T.P. Speed, Summaries of Affymetrix GeneChip probe level data, Nucleic Acids Res. 31 (2003) e15, https://doi.org/10.1093/nar/gng015.
[15] W.E. Johnson, C. Li, A. Rabinovic, Adjusting batch effects in microarray expression data using empirical Bayes methods, Biostatistics 8 (2007) 118–127, https://doi.org/10.1093/biostatistics/kxj037.
[16] J.T. Leek, J.D. Storey, Capturing heterogeneity in gene expression studies by surrogate variable analysis, PLoS Genet. 3 (2007) 1724–1735, https://doi.org/10.1371/journal.pgen.0030161.
[17] B.H. Mecham, P.S. Nelson, J.D. Storey, Supervised normalization of microarrays, Bioinformatics 26 (2010) 1308–1315, https://doi.org/10.1093/bioinformatics/btq118.
[18] G.K. Smyth, Limma: linear models for microarray data, in: R. Gentleman, V. J. Carey, W. Huber, R.A. Irizarry, S. Dudoit (Eds.), Bioinformatics and Computational Biology Solutions Using R and Bioconductor, Springer, New York, 2005, pp. 397–420.
[19] A. Dobin, C.A. Davis, F. Schlesinger, et al., STAR: ultrafast universal RNA-seq aligner, Bioinformatics 29 (2013) 15–21, https://doi.org/10.1093/bioinformatics/bts635.
[20] B. Li, C.N. Dewey, RSEM: accurate transcript quantification from RNA-Seq data with or without a reference genome, BMC Bioinf. 12 (2011) 323, https://doi.org/10.1186/1471-2105-12-323.
[21] M.I. Love, W. Huber, S. Anders, Moderated estimation of fold change and dispersion for RNA-seq data with DESeq2, Genome Biol. 15 (2014) 550, https://doi.org/10.1186/s13059-014-0550-8.
[22] J.M.S. Chan, P.S. Jin, M. Ng, et al., Development of molecular magnetic resonance imaging tools for risk stratification of carotid atherosclerotic disease using dual-targeted microparticles of iron oxide, Transl Stroke Res 13 (2022) 245–256, https://doi.org/10.1007/s12975-021-00931-3.
[23] J.M. Chan, S.J. Park, M. Ng, W.C. Chen, J. Garnell, K. Bhakoo, Predictive mouse model reflects distinct stages of human atheroma in a single carotid artery, Transl. Res. 240 (2022) 33–49, https://doi.org/10.1016/j.trsl.2021.08.007.
[24] S. Anders, P.T. Pyl, W. Huber, HTSeq-A Python framework to work with high-throughput sequencing data, Bioinformatics 31 (2015) 166–169, https://doi.org/10.1093/bioinformatics/btu638.
[25] M.D. Robinson, D.J. McCarthy, G.K. Smyth, edgeR: a Bioconductor package for differential expression analysis of digital gene expression data, Bioinformatics 26 (2010) 139–140, https://doi.org/10.1093/bioinformatics/btp616.
[26] D.D. Smith, X. Tan, O. Tawfik, G. Milne, D.J. Stechschulte, K.N. Dileepan, Increased aortic atherosclerotic plaque development in female apolipoprotein E-null mice is associated with elevated thromboxane A2 and decreased prostacyclin production, J. Physiol. Pharmacol. 61 (2010) 309–316.
[27] Y. Nakashima, A.S. Plump, E.W. Raines, J.L. Breslow, R. Ross, ApoE-deficient mice develop lesions of all phases of atherosclerosis throughout the arterial tree, Arterioscler. Thromb. 14 (1994) 133–140, https://doi.org/10.1161/01.atv.14.1.133.
[28] M.E. Rosenfeld, M.M. Averill, B.J. Bennett, S.M. Schwartz, Progression and disruption of advanced atherosclerotic plaques in murine models, Curr. Drug Targets 9 (2008) 210–216, https://doi.org/10.2174/138945008783755575.
[29] S. Li, Y. Peng, X. Wang, et al., Cardiovascular events and death after myocardial infarction or ischemic stroke in an older Medicare population, Clin. Cardiol. 42 (2019) 391–399, https://doi.org/10.1002/clc.23160.
[30] R.K. Akyea, J. Kai, N. Qureshi, B. Iyen, S.F. Weng, Sub-optimal cholesterol response to initiation of statins and future risk of cardiovascular disease, Heart 105 (2019) 975–981, https://doi.org/10.1136/heartjnl-2018-314253.
[31] J. Rockberg, L. Jørgensen, B. Taylor, P. Sobocki, G. Johansson, Risk of mortality and recurrent cardiovascular events in patients with acute coronary syndromes on high intensity statin treatment, Prev Med Rep 6 (2017) 203–209, https://doi.org/10.1016/j.pmedr.2017.03.001.
[32] J.W. Williams, L.H. Huang, G.J. Randolph, Cytokine circuits in cardiovascular disease, Immunity 50 (2019) 941–954, https://doi.org/10.1016/j.immuni.2019.03.007.
[33] P. Libby, G.K. Hansson, From focal lipid storage to systemic inflammation: JACC Review Topic of the Week, J. Am. Coll. Cardiol. 74 (2019) 1594–1607, https://doi.org/10.1016/j.jacc.2019.07.061.
[34] V. Bhaskar, J. Yin, A.M. Mirza, et al., Monoclonal antibodies targeting IL-1 beta reduce biomarkers of atherosclerosis in vitro and inhibit atherosclerotic plaque formation in Apolipoprotein E-deficient mice, Atherosclerosis 216 (2011) 313–320, https://doi.org/10.1016/j.atherosclerosis.2011.02.026.
[35] T.X. Zhao, Z. Mallat, Targeting the immune system in atherosclerosis: JACC State-of-the-Art Review, J. Am. Coll. Cardiol. 73 (2019) 1691–1706, https://doi.org/10.1016/j.jacc.2018.12.083.
[36] D. Gomez, R.A. Baylis, B.G. Durgin, et al., Interleukin-1β has atheroprotective effects in advanced atherosclerotic lesions in mice, Nat. Med. 24 (2018) 1418–1429, https://doi.org/10.1038/s41591-018-0124-5.
[37] B.M. Everett, J.H. Cornel, M. Lainscak, et al., Anti-Inflammatory therapy with Canakinumab for the prevention of hospitalization for heart failure, Circulation 139 (2019) 1289–1299, https://doi.org/10.1161/CIRCULATIONAHA.118.038010.
[38] P.M. Ridker, B.M. Everett, T. Thuren, et al., Antiinflammatory therapy with Canakinumab for atherosclerotic disease, N. Engl. J. Med. 377 (2017) 1119–1131, https://doi.org/10.1056/NEJMoa1707914.
[39] B.M. Everett, A.D. Pradhan, D.H. Solomon, et al., Rationale and design of the Cardiovascular Inflammation Reduction Trial: a test of the inflammatory hypothesis of atherothrombosis, Am. Heart J. 166 (2013) 199–207, https://doi.org/10.1016/j.ahj.2013.03.018, e15.
[40] Y.H. Yoon, J.M. Ahn, D.Y. Kang, et al., Impact of SYNTAX Score on 10-year outcomes after revascularization for left main coronary artery disease, JACC Cardiovasc. Interv. 13 (2020) 361–371, https://doi.org/10.1016/j.jcin.2019.10.020.
[41] G. Sianos, M.A. Morel, A.P. Kappetein, et al., The SYNTAX Score: an angiographic tool grading the complexity of coronary artery disease, EuroIntervention 1 (2005) 219–227.
[42] L. Zhuo, X. Chen, Y. Sun, et al., Rapamycin inhibited pyroptosis and reduced the release of IL-1β and IL-18 in the septic response, BioMed Res. Int. 2020 (2020), 5960375, https://doi.org/10.1155/2020/5960375.
[43] T.H. Lin, W.L. Lee, W.J. Lee, W.H. Sheu, Y.C. Liao, K.W. Liang, Dyslipidemia, not inflammatory markers or adipokines, contributes significantly to a higher SYNTAX Score in stable coronary artery disease (from the Taichung CAD study), Acta Cardiol. Sin. 37 (2021) 232–238, https://doi.org/10.6515/ACS.202105_37(3).20201116B.
[44] W. Xu, H. Guan, D. Gao, et al., The association of Syntax Score with levels of lipoprotein(a) and inflammatory biomarkers in patients with stable coronary artery disease and different low-density lipoprotein cholesterol levels, Diabetes Metab Syndr Obes 13 (2020) 4297–4310, https://doi.org/10.2147/DMSO.S279814.
[45] S. Rajpal, M.A. Rana, E. Peter, et al., Relationship of Syntax Score with markers of vascular inflammation, J. Am. Coll. Cardiol. 63 (2014) A2066, https://doi.org/10.1016/S0735-1097(14)62069-6.
[46] Z. Hu, W. Liu, X. Hua, et al., Single-cell transcriptomic atlas of different human cardiac arteries identifies cell types associated with vascular physiology, Arterioscler. Thromb. Vasc. Biol. 41 (2021) 1408–1427, https://doi.org/10.1161/ATVBAHA.120.315373.
[47] V. Sorokin, K. Vickneson, T. Kofidis, et al., Role of vascular smooth muscle cell plasticity and interactions in vessel wall inflammation, Front. Immunol. 11 (2020), 599415, https://doi.org/10.3389/fimmu.2020.599415.
[48] A. Kuzan, J. Wisniewski, K. Maksymowicz, M. Kobielarz, A. Gamian, A. Chwilkowska, Relationship between calcification, atherosclerosis and matrix proteins in the human aorta, Folia Histochem. Cytobiol. 59 (2021) 8–21, https://doi.org/10.5603/FHC.a2021.0002.
[49] T. Chiong, E.S. Cheow, C.C. Woo, et al., Aortic wall extracellular matrix proteins correlate with Syntax Score in patients undergoing coronary artery bypass surgery, Open Cardiovasc. Med. J. 10 (2016) 48–56, https://doi.org/10.2174/1874192401610010048.